Noisy cell growth rate leads to fluctuating protein concentration in bacteria

Saburo Tsuru[1]**, Junya Ichinose**[2]**, Akiko Kashiwagi**[1,5]**, Bei-Wen Ying**[1]**, Kunihiko Kaneko**[2,3] **and Tetsuya Yomo**[1,2,4,6]

[1] Department of Bioinformatic Engineering, Graduate School of Information Science and Technology, Osaka University, 2-1 Yamadaoka, Suita, Osaka 565-0871, Japan
[2] Exploratory Research for Advanced Technology (ERATO), Japan Science and Technology Agency (JST), 1-5 Yamadaoka, Suita, Osaka 565-0871, Japan
[3] Department of Pure and Applied Sciences, University of Tokyo, Komaba, Meguro-ku, Tokyo 153-8902, Japan
[4] Graduate School of Frontier Biosciences, Osaka University, 2-1 Yamadaoka, Suita, Osaka 565-0871, Japan

E-mail: yomo@ist.osaka-u.ac.jp

Abstract

The present study discusses a prime cause of fluctuating protein concentrations, which play a significant role in generating phenotypic diversity in bacteria. A genetic circuit integrated in a bacterial genome was used to evaluate the cell-to-cell variation in protein concentration. A simple dynamic model, comprising terms for synthesis and dilution, was used to elucidate the contributions of distinct noises to the fluctuation in cell protein concentration. Experimental and theoretical results demonstrated that noise in the rate of increase in cell volume (cell growth rate) serves as a source of extrinsic noise that accounts for dozens of percent of the total noise, whereas intrinsic noise in protein synthesis makes only a moderate contribution to the fluctuation in protein concentration. This suggests that such external noise in the cell growth rate has a global effect on cellular components, resulting in a large fluctuation in protein concentration in bacterial cells.

S This article has associated online supplementary data files

Introduction

There can be significant variation in cell volume, protein number, etc, within a population of genetically identical cells, caused by the stochastic biological reactions occurring inside these cells. Large fluctuations in cell protein concentration can result in phenotypic diversity [13, 20, 24, 30], and is considered to play an important role in the biological processes of differentiation, development, adaptation and evolution [1, 17, 19, 21, 23, 33, 36].

The dynamics of cell protein concentration can be described conceptually as a balance between positive and negative factors: synthesis due to gene expression and regulation, and dilution due to an increase in cell volume (cell growth rate) and protein degradation [2]. The stochastic fluctuation of synthesis and dilution is consequently attributable to the cell-to-cell variation in protein concentration. Such inherent variability in cell protein concentration, as widely reported, is largely determined by 'intrinsic' noise that comprises the stochastic fluctuation of transcription and translation of individual genes and the specific degradation of their products [9, 13, 15, 27, 37, 41], and the unclear 'extrinsic' noise, which has a global effect on all cellular components [11, 13, 26, 29, 40]. Many studies have focused on the so-called intrinsic and extrinsic noises involved in protein synthesis, but there is little literature related to protein dilution. As fluctuation in protein concentration can

be generated by both noisy synthesis and noisy dilution, we focus on the dilution rate to evaluate the noise that it potentially contributes to fluctuation in protein concentration.

In bacteria, protein dilution is governed by an increase in cell volume within a single generation, rather than protein degradation [2, 31]. The rate of increase in cell volume can be considered as the dilution rate; consequently, noise in the cell growth rate makes a dominant contribution to noisy dilution. Since the cell growth rate, in principle, has a global effect on the whole cell, its noise can be defined as a source of extrinsic noise. To isolate this possible extrinsic noise, we constructed a genetic circuit within a bacterial genome, and analysed the cell-to-cell variations in protein concentration and the increase in cell volume. We found that noise in the synthesis rate (gene expression) played only a modest part in the fluctuation in protein concentration in the cells. Instead, we found considerable cell-to-cell variation in cell volume (cell growth rate), which suggests that noise in the cell growth rate might have a global effect on the fluctuation in cell protein concentration. We used a simple dynamic model, comprising terms for synthesis and dilution, to elucidate the contribution of distinct noises to the fluctuation in cell protein concentration. Experimental and theoretical investigations confirmed that noise in the cell growth rate serves as a source of extrinsic noise, contributing to the total noise, accounting for dozens of percent.

Materials and methods

Genetic construction

The gene *cat*, encoded chloramphenicol acetyltransferase, was amplified from the plasmid pPROtetEM7-zeocin (Clontech) using the primers CmApaI-f (5′-GGGCCCAGGAAGCTAAAATGGAGAA-3′) and CmApaI-r (GGGCCCTTACGCCCCGCCCTGCCAC-3′), followed by subcloning into the plasmid pCR2.1-TOPO (Invitrogen). The constructed plasmid pCR2.1-TOPO-cat was digested with *Apa*I, and the resulting *cat* fragment was inserted into the plasmid pT3 (DDBJ AB434476), a derivative of pT1 (DDBJ AB434474), whose *Eco*RV site was changed to the *Apa*I site. The *cat* gene, fused to a homogeneous sequence for genome recombination, was amplified from the resulting plasmid pT3-cat using the primers chgalkl (5′-AAGCCCACGTTTTACGGATC-3′) and reG(I)l-kmr (5′-GCTCCGTTCAACTAGCAGAC-3′). The resulting PCR (polymerase chain reaction) fragment was integrated into the genome (downstream of *gfpuv5*) of the *Escherichia coli* cells, strain OSU11 [18], whose *galK* and *intC* genes had been replaced with the sequences PtetA-*gfpuv5* and Ptrc-*dsred.t4-tetR-zeo*r, respectively. The resulting strain was designated OSU12-*cat*, and the cells were examined by flow cytometry. DNA sequences of the *galK* locus of the OSU12-*cat* strain are available in DDBJ under the accession number AB434473. Cells carrying a similar core circuit (PtetA-*gfpuv5* and Ptrc-*dsred.t4-tetR-cat*), designated OSU10 [18], were used for time-lapse microscopy. Homogeneous

replacement based on the *red* system was performed to construct the genome-integrated synthetic circuit, as described in a previous report [10].

Cell growth medium

Escherichia coli cells were grown in a modified M63 (mM63) medium (62 mM K_2HPO_4, 39 mM KH_2PO_4, 15 mM $(NH_4)2SO_4$, 2 μM $FeSO_4 \bullet 7H_2O$, 15 μM thiamine hydrochloride, 203 μM $MgSO_4 \bullet 7H_2O$ and 22 mM glucose) as the minimal medium. Cells were grown in the mM63 medium at 37 °C (32 °C for the OSU10 strain) for several passages until the growth rate became stable.

Gene expression

Bacterial cells were grown in the mM63 medium supplied with 10 μM IPTG (isopropyl-β-D-thiogalactopyranoside) for 18 h to induce full expression of RFP (red fluorescent protein) at 37 °C. Subsequently, the exponentially growing cells were inoculated in the same medium with the addition of doxycycline hydrochloride (Dox) to induce the expression of GFP (green fluorescent protein). The initial cell concentration was 10^4 cells mL^{-1}, and the final concentrations of Dox were 16.7, 22.5, 33.7, 45 and 113 nM. Cultures were sampled every 2 h.

Measurement by flow cytometry

Gene expression (fluorescence intensity) and cell volume were evaluated using a flow cytometer (FACSAria cell sorter; Becton Dickinson) with a 488 nm argon laser, a 515–545 nm emission filter (GFP) and a 563–589 nm emission filter (RFP) at a medium flow rate. The following PMT voltage settings were applied: 203 (forward scatter, FSC), 440 (side scatter), 615 (GFP) and 593 (RFP). At least 3000 cells were collected for each measurement. Cell samples mixed with fluorescent beads (Floresbrite YG Microspheres, 2 μm; Polysciences Inc.) were loaded for the calculation of cell concentration.

Data analysis

The flow data were converted to TXT format. The cellular protein (GFP or RFP) concentration was calculated by dividing the fluorescence value (green or red fluorescence) by the FSC value [22, 33] using MATLAB (MathWorks, Natick, MA). Autofluorescence was subtracted. The systematic error resulting from events that occurred at the bottom or top of the instrument's range was eliminated. One percent of the total number of cells (events) from both the highest and the lowest values of fluorescence intensity were removed to prevent unreliable rare events. Gate size was defined by a narrow FSC window centred about the FSC mean (figure 1(*b*)). We used a width chosen to achieve a substantial reduction in the coefficient of variation (CV) (figure S5; stacks.iop.org/PhysBio/6/036015), while maintaining a sufficient number of cells (440–540).

To calculate the total number of GFPs per single cell from the relative green fluorescence intensity, we used standard
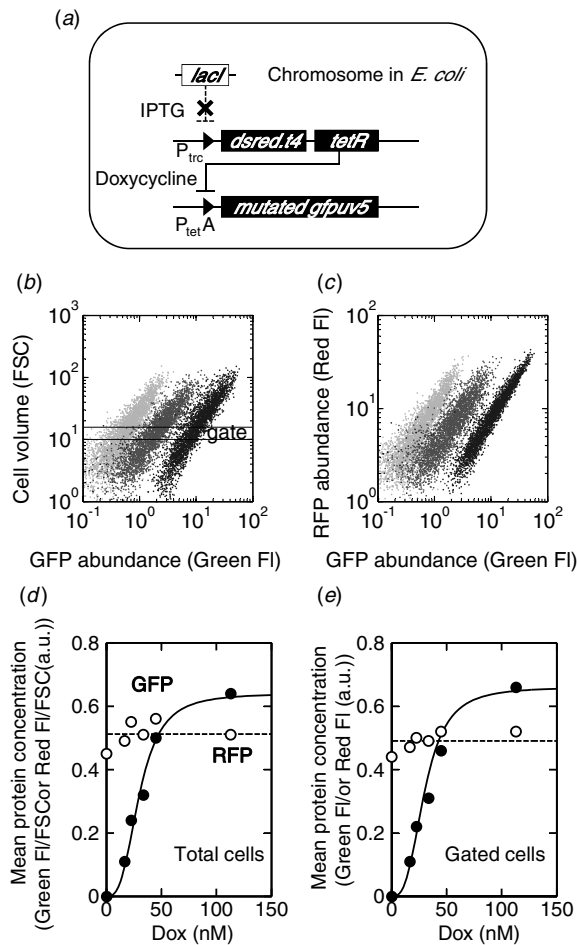
Figure 1. Properties of the genetic circuit. A genetic circuit was constructed and integrated into the *E. coli* chromosome for the regulation of synthesis of the featured protein (*a*). The PtetA promoter, which controls the expression of mutated *gfpuv*5, is regulated by the repressor protein TetR and the inducer doxycycline (Dox). The expression of TetR is controlled by the endogenous LacI and the additional IPTG. The expression levels of GFP and RFP, and the corresponding cell volumes, were measured at the single-cell level in the presence of 0, 16.7 and 113 nM Dox, respectively ((*b*) and (*c*)). The averaged protein concentration was plotted against Dox concentration for total (*d*) and gated (*e*) cells of a specific cell volume ((*b*), gated region). Open and closed circles show the mean concentrations of RFP and GFP, respectively. The solid (fitted by a Hill-type function for GFP) and broken (mean for RFP) lines are indicated for guidance.

beads (Living Colors EGFP Calibration Beads; Clontech) according to manufacturer's protocol. The results showed that each GFP had a fluorescence intensity of $10^{-3.3}$ arbitrary units. The total number of GFPs per single cell was calculated by multiplying the relative GFP concentration by the relative cell volume, FSC, the average value of which was 13 arbitrary units, and then dividing it by $10^{-3.3}$.

Cell culture under a microscope and image acquisition

Cultures (OSU10) were grown overnight in the mM63 medium containing 1 mM IPTG and 250 nM Dox at 32 °C. Cells in the logarithmic growth phase (2 μl of culture) were placed on a glass coverslip and immersed in the same medium as that

used for the preculture, and subsequently covered with a thin polyacrylamide gel (5%) to prevent suspension of cell growth. Fluorescence images were acquired at 240× magnification using a fluorescence microscope (TE2000; Nikon) and a cooled CCD camera (DV887; Andor). Time-lapse images of various fields were automatically recorded every 5 min using the Metamorph microscope control software (Molecular Devices Corporation, Dawningtown, PA).

Image analysis

Time-series images of RFP fluorescence were used to analyse the increase in cell volume. We considered cell length as cell volume because every cell was rod shaped. Shapes of camera-captured cells were outlined manually, and cell volume was calculated according to a method reported previously [39]. Growing cells, whose volumes increased exponentially within a single generation (from birth to division), were collected randomly. Cell growth rates were obtained by calculating the slope of the temporal increase in cell volume on a logarithmic scale (figure 5(*b*)) for ~260 division events independently.

Results and discussion

Architecture of chromosomally integrated gene circuits

An *E. coli* cell harbouring a cascaded gene circuit (figure 1(*a*)) in its chromosome was constructed for experimental measurements and noise classification. Because inherent prokaryotic promoters exhibit diverse architectures in complex cellular networks, a synthetic gene regulatory circuit was designed for the seamless tuning of the gene expression [12, 32], according to a well-established design principle [29]. Both the reporter gene, *gfp* [16], for the quantitative detection of cell protein concentration, and the repressor gene, *tetR*, for the regulative expression of *gfp*, were integrated into the chromosome to minimize noise in the copy number of DNA molecules. The expression of the Tet repressor was monitored by the other reporter gene, *rfp* [7], which was co-expressed with *tetR*. A constant expression level of *tetR*, regardless of the expression level of *gfp*, can be guaranteed by this genetic design, as noise in the native expression of LacI, which controls the promoter Ptrc, can be eliminated when sufficient IPTG is present (see supplementary data: stacks.iop.org/PhysBio/6/036015). As described previously [11, 29], full induction of an upstream gene can prevent the transmission of its own expression noise to a downstream gene, so that only the network-independent noise, i.e. global noise, occurs.

Cells were grown in the presence of 10 μM IPTG with various concentrations of Dox (0–113 nM), resulting in a wide-ranging expression level of *gfp*. The intensity of green (Green FI) and red (Red FI) fluorescence of each cell, representing the abundance of GFP and RFP expressed in a single cell, and the FSC of each cell particle, which is related to cell volume (data not shown) [8], were measured using a flow cytometer. A genetically identical cell population under a widely used culture condition (see materials and methods section) exhibited a broad distribution (approximately two orders of magnitude)
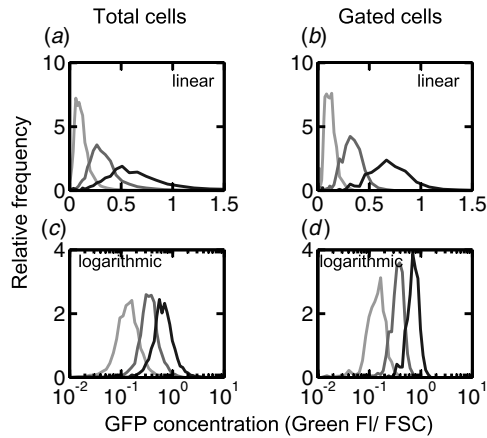
Figure 2. Steady-state distributions of cellular GFP concentrations. Steady-state distributions of cellular GFP concentration was obtained at Dox concentrations of 16.7, 33.7 and 113 nM (left–right). Distributions of total ((*a*) and (*c*)) and gated ((*b*) and (*d*)) cells are plotted on both linear ((*a*) and (*b*)) and logarithmic ((*c*) and (*d*)) scales.
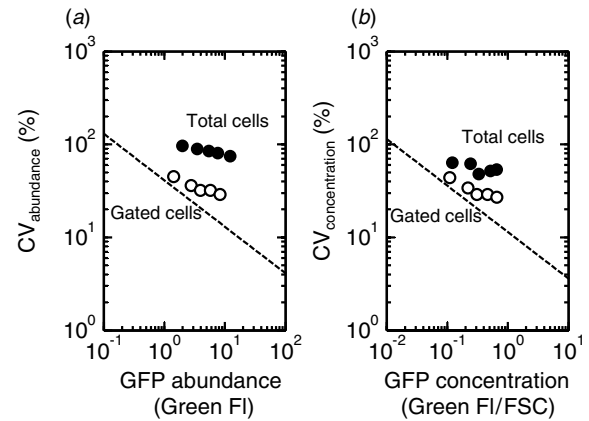

Figure 3. Relative fluctuations during steady state. The relative fluctuation CV (standard deviation divided by mean) in cellular protein abundance (*a*) and cell protein concentration (*b*) for total (closed circles) and gated (open circles) cells was plotted. Circles from left to right represent CV in the presence of 16.7, 22.5, 33.7, 45 and 113 nM Dox.

of both protein (GFP and RFP) abundance and cell volume (figures 1(*b*) and (*c*)). The abundance of GFP (Green FI) was correlated to cell volume (FSC), with a slope of approximately 1 on a logarithmic scale, regardless of the expression level of GFP induced by Dox (figure 1(*b*)). In addition, the intensity of GFP was proportional to that of RFP (figure 1(*c*)), which implies that the protein abundance in the cell was related to cell volume.

Subsequently, the average protein concentration of the cell population was analysed. The relative protein concentration was calculated in two ways to prevent confusion caused by the different approaches in data analysis. One method was simply to take the ratio of Green FI (or Red FI) to FSC for the whole cell population [22, 33], considering the correlation between GFP abundance and cell volume. The other method was to directly use the Green FI (or Red FI) value of a subpopulation gated within a narrow region of FSC as a defined cell volume, as described previously [5, 26, 40]. No significant difference was found in the average concentration (mean value) acquired with the two approaches (figures 1(*d*) and (*e*): total and gated cells, respectively). The average GFP concentration (closed circles) of the cell population, either total or gated, increased with the concentration of the inducer Dox, whereas the average RFP concentration (open circles) remained constant (figures 1(*d*) and (*e*)). This implies that the desired outcome of the genetic construction was achieved.

Distribution of cell protein concentration

Protein concentration of single cells showed a broad distribution, indicating considerable cell-to-cell variation (figure 2). Unlike the average concentration for the population, the two approaches (total and gated) gave dissimilar shapes for the distribution of GFP concentration. The distribution of total cells showed a long right tail on the linear scale (figure 2(*a*)) and a normal tail on the logarithmic scale

(figure 2(*c*)). In contrast, the distribution of gated cells exhibited a normal-appearing shape on both linear and logarithmic scales (figures 2(*b*) and (*d*)).

Further analysis was performed to determine whether the different shapes of the distributions obtained using the two approaches would result in a clear conclusion. The ratio of the standard deviation to average GFP abundance and concentration (CV) was plotted against the average GFP abundance and concentration, respectively (figure 3). Both CV values (abundance and concentration) of the gated cells (open circles) declined slightly with increasing GFP (mean value). Nevertheless, the slope of the decline was not as sharp as that expected from the Poissonian stochastic process (slope value 0.5, broken lines in figure 3), which can be interpreted as stochasticity of both the expression reactions from the gene to the protein [9, 13, 15, 27, 37, 41] and the partition error of the protein from the mother to the daughter cell during cell division [32]. Moreover, the CV of total cells (closed circles) exhibited an approximately constant value, regardless of the amount of GFP in cells. Neither total nor gated cells showed any considerable decrease in the variance of GFP, leading to the conclusion that a steady fluctuation in cell protein concentration exists in both cases. The independence of the CV from the expression level and the right-tailed distribution have been reported previously [5, 6, 13, 14, 22, 26, 29], but remained unclear because of the unknown source of extrinsic noise [28].

Noise in the cell growth rate as a source of fluctuation in protein concentration

To identify the element that maintains the fluctuation in cell protein concentration in bacterial cells, we considered the dynamics of protein concentration as consisting of two processes, synthesis and dilution, as in the following equation:

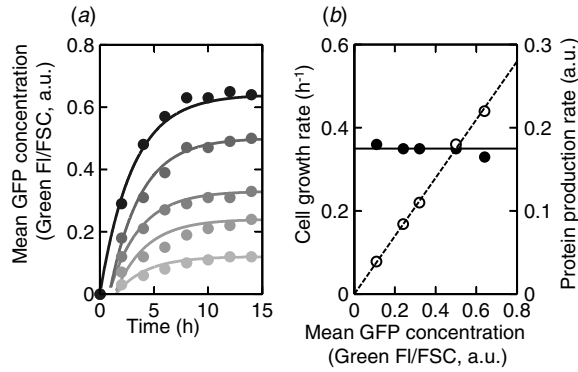$$\frac{\mathrm{d}x}{\mathrm{d}t} = k_x - \mu x, \qquad (1)$$

Figure 4. Temporal changes in protein concentration characterized by cell growth rate. Temporal changes in mean concentrations were evaluated experimentally (*a*) in the presence of Dox concentrations of 16.7, 22.5, 33.7, 45 and 113 nM (closed circles from light grey to dark grey). Solid lines represent a single exponential relaxation (equation (3.1)) according to the cell growth and synthesis rates shown in panel (*b*). Cell growth rates under the various conditions (closed circles in panel (*b*)) show a mean value of 0.35 h^{-1} (solid line). Protein synthesis rates (open circles in (*b*)) are plotted in a similar way. Data on total cells were used for this analysis because the distribution of total cells was not affected by the method of gating and maintained a clear log-normal shape (figure 2).

where x, k_x and μ represent the protein concentration, protein synthesis rate and rate of increase in cell volume, respectively. This simple standard description has been previously used to interpret various biological phenomena successfully [2, 27, 31], and the basic concepts of the model considering mRNA step are described in the supplementary data: stacks.iop.org/PhysBio/6/036015. Protein synthesis is controlled by the protein synthesis rate k_x, which is constant against time, because the synthesis rate is determined by the concentration of Dox, which activates the promoter PtetA and raises the expression level of GFP. Protein dilution is controlled by both protein degradation and increase in cell volume. In a growing bacterial cell, the rate of non-specific protein degradation is slow enough to be ignored [25], compared with the rate of increase in cell volume. Thus, protein dilution is mostly due to the cell growth rate μ, and the steady protein concentration x should be calculated as the ratio of the protein synthesis rate k_x to the cell growth rate μ.

To verify the conceptual dynamic model (equation (1)), the temporal change in cellular GFP concentration was examined experimentally. The results showed that the mean GFP concentration gradually approached a final steady-state value governed by the concentration of Dox (figure 4(*a*), closed circles). Such gradual relaxation to a steady state can be anticipated from the analytical solution of equation (1):

$$\frac{dx}{dt} = -\mu \left(x - \frac{k_x}{\mu} \right). \tag{2}$$

The relaxation rate seems to be decided by the cell growth rate μ, and the final protein concentration at the steady state x_{st} is supposed to reach a value of $\frac{k_x}{\mu}$. The analytical solution can be described explicitly as follows:

$$x(t) = x_{st} - (x_{st} - x(0)) \, e^{-\mu t}, \tag{3.1}$$

$$x_{st} = \frac{k_x}{\mu}. \tag{3.2}$$

To examine whether the relaxation of protein concentration can be explained by equation (3.1), the temporal changes in GFP concentration (figure 4(*a*)) and cell growth rate (figure 4(*b*)) were investigated. The cell growth rate was determined from the rate of the increase in cell number, which was identical to that of the increase in cell volume at the logarithmic growth phase [2]. As shown in figure 4, the cell growth rate remained stable in spite of the changing concentrations of Dox that induced the GFP expression (figure 4(*b*), closed circles). The average μ (mean value, figure 4(*b*), solid line), 0.35 h^{-1}, was used to estimate individual values of synthesis rate k_x (figure 4(*b*), open circles), corresponding to the average GFP concentrations. Consequently, these estimated values (μ and k_x) were used to reconstitute the temporal dynamics of protein concentration. Intriguingly, the reconstituted relaxation curves all fitted the experimental observation perfectly (figure 4(*a*), solid lines), despite the cell growth rate determined from the increase in cell number. This demonstrates that protein dilution was controlled by the cell growth rate, and the simple model (equations (1) and (2)) precisely captured the dynamic changes in cell protein concentration. Note that the rate of increase in cell number is equal to that of cell volume during the steady exponential period [2].

According to the dynamic model (equation (1)), fluctuation in cell protein concentration can arise from noise either in synthesis (due to gene expression) or dilution (due to cell growth). There has been much research on noise in protein synthesis [9, 15, 41], whereas noise in protein dilution has not yet been clearly explained. Here, we considered the potential noise involved in protein dilution, that is, noise in the cell growth rate [34], and attempted to answer the question of the extent to which noise in the cell growth rate contributes to the large fluctuation in cell protein concentration.

Noise in the cell growth rate function plotted in a multiplicative manner against protein concentration (μx in equation (1)) is prospectively attributable to the fluctuation in cell protein concentration. We captured ~260 division events (cell cycles) directly at the single-cell level by time-lapse microscopy to observe how noisy the cell growth rate could be. Cells that started exponential growth without a detectable lag phase and continued to divide for several generations were selected and used in the analysis (figure 5(*a*)). The rate of increase in cell volume (corresponding to cell length) in each single generation was recorded, as shown in figure 5(*b*). For instance, a cell of a slower growth rate (e.g. 0.47) would stochastically grow faster (e.g. 0.54) after a certain time and vice versa for other cell lines. Such fluctuation in the growth rate of individual cells over time causes cell-to-cell variations in the cell growth rate, as represented in figure 5(*c*). The distribution of the cell growth rate, including a total of ~260 division events (cell cycles), exhibited marked fluctuation (figure 5(*c*)), with a standard deviation of ~13% around an average of ~0.45 h^{-1}. This indicates that noise in the cell growth rate had reached a considerable level, ~13% per generation. Such
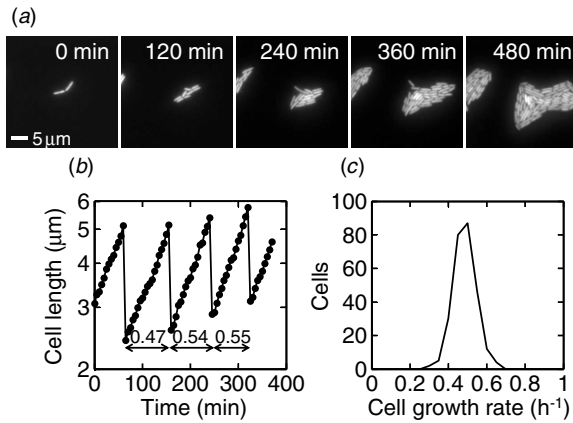
Figure 5. Time-lapse microscopic observations of growing cells. Noise in the rate of increase in cell volume was measured directly by observing growing cells, shown as the snapshots of growing bacterial cells (*a*). Temporal changes in cell length were traced at the single-cell level (*b*). Time-lapse images were automatically recorded every 5 min. Cell growth rates (h^{-1}) within a single generation are indicated. The cell growth rates, observed from ~260 division events, displayed a Gaussian-like distribution with a CV of 13% (*c*).

Figure 6. Relationship between distributions of cell growth rate and protein concentration. The distribution of cell growth rate ($\hat{P}(\mu)$, white distribution) was transformed to the distribution of protein concentration ($P(x)$, light- and dark-shaded distributions, arranged vertically) according to the curve $x = \frac{k_x}{\mu}$ (solid lines), as indicated by broken arrows. The protein synthesis rate k_x was amplified from 0.11 to 0.22 (light and dark lines, respectively) in the presence of Dox concentrations increasing from 33.7 to 113 nM, leading to a shift in the distribution of protein concentration from $P(x_1)$ (light shading) to $P(x_2)$ (dark shading).

cell-to-cell variations in growth rate among a cell population, similar as those in the gene expression [13, 41], do represent the difference over time but not in steady state.

Contribution of noise in the cell growth rate to fluctuation in protein concentration

How is such a high level of noise in the cell growth rate involved in the fluctuation in protein concentration? According to the dynamic model (equation (1)), the steady state of cell protein concentration is inversely correlated to the cell growth rate (equation (3.2)). When the rate of increase in cell volume varies among cells, the steady GFP concentration of each cell x can be determined from the relation $x = \frac{k_x}{\mu}$, and forms a distribution. Such transformation from cell growth rate to protein concentration is schematically expressed by the curve $x = \frac{k_x}{\mu}$ (figure 6, solid lines). The corresponding mathematical procedure is described in the supplementary data: stacks.iop.org/PhysBio/6/036015. For instance, in the presence of 33.7 and 113 nM Dox, the protein synthesis rate k_x was 0.11 and 0.22, respectively (figure 4(*b*)), resulting in two corresponding dynamic curves (light and dark lines). The distribution of the cell growth rate, $\hat{P}(\mu)$, acquired from the experimental data, displayed an average of 0.35 h^{-1} and a CV$_\mu$ of 13%, and was transformed to the distribution of the protein concentration $P(x)$ (the theoretical procedure in the supplementary data: stacks.iop.org/PhysBio/6/036015). Once the protein synthesis rate k_x was raised from 0.11 to 0.22 (an increase of approximately two-fold) as a result of the increasing Dox concentration (from 33.7 to 113 nM), the distribution of protein concentration was shifted from $P(x_1)$ (light shading in figure 6) to $P(x_2)$ (dark shading), corresponding to the identical $\hat{P}(\mu)$ (figure 6). As a result, both the averaged protein concentration (mean value) and the standard deviation were approximately doubled, from 0.31 to 0.63 and from 0.044
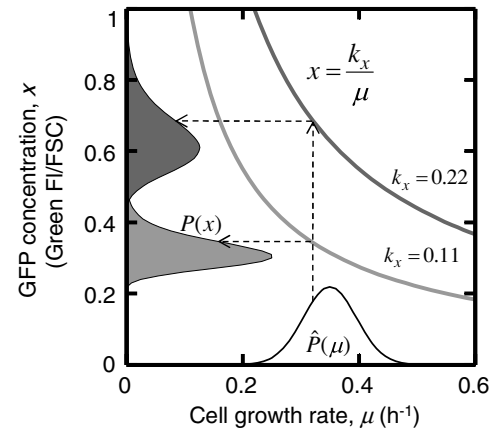
to 0.088, respectively. The CV$_x$ of both distributions was calculated; it was approximately equal to 14%, independent of the expression level. This indicates that the fluctuation in protein concentration (CV$_x$) transformed from the cell growth rate ($\hat{P}(\mu)$) was not determined by the protein concentration (mean value of x) itself but by the shape of the distribution $\hat{P}(\mu)$. Because the slope of $x = \frac{k_x}{\mu}$ becomes steep when the cell growth rate decreases, a wider distribution of the protein concentration with a longer right tail can be obtained at a higher concentration (figure 6, broken arrows), similar to what is shown in figure 2 [14]. Thus, such independence of CV$_x$ with respect to the expression level is well explained by the dilution effect of cell growth rate on protein concentration. In addition, the present analysis was based on the assumption of a steady state with a slow noise limit, though a white noise limit led to the same conclusion (see supplementary data: stacks.iop.org/PhysBio/6/036015). We assumed that the protein synthesis rate and the cell growth rate were decoupled. However, if the protein synthesis rate increased in proportion to the growth rate, the change in protein concentration due to the growth rate would be cancelled out; resultantly, the fluctuation of protein concentration caused by noise in the growth rate would be irrelevant. Actually, we have observed that the protein concentration increased significantly once the GFP distribution was at a steady state with a slower growth (data not shown). As the growth-rate independent part and the proportional part equally contribute to the protein synthesis, the fluctuation due to the noisy growth rate is not cancelled out.

We next determined how noise in the cell growth rate contributed to the fluctuation in protein concentration (figure 7). We estimated extrinsic noise by fitting a commonly used equation (A.5.3) (solid curves). The observed total noise was divided into the intrinsic and extrinsic noises; resultantly,
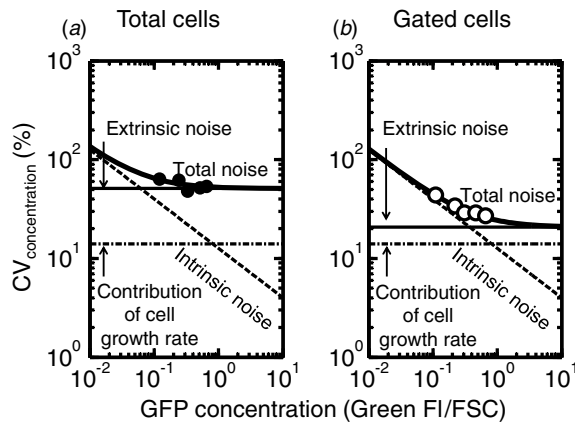
Figure 7. Composition of fluctuation in protein concentration. The total fluctuation (equation (A.5.3) thick line) for total (*a*) and gated (*b*) cells was composed of intrinsic noise (broken lines) and extrinsic noise (horizontal solid lines). Each contribution is detailed in the appendix. The contribution of intrinsic noise was estimated by expanding the dual colour system and is detailed in the supplementary data. The circles represent a replotting of figure 3(*b*). Noise in the cell growth rate (horizontal chain lines) contributes a constant 14%, as part of extrinsic noise, accounting for a proportion of the entire extrinsic noise, constituting dozens of percent (68% and 27% for gated and total cells, respectively).

the total extrinsic noise was 51% or 21% (CV for total and gated cells, respectively) (horizontal solid lines). As noise in the cell growth rate constantly generates a 14% CV for protein concentration (horizontal chain lines), it is estimated to account for 27% and 68% of the total extrinsic noise for total and gated cells, respectively. Apparently, noise in the cell growth rate shares a considerable fraction of extrinsic noise that causes the fluctuation in protein concentration. Note that the CV of GFP (or RFP) distribution keeps constant regardless of the shape of GFP (or RFP) distribution that may change due to the mean or shape of the cell growth rate.

In addition, to compare the contribution of noise in the cell growth rate with that of the intrinsic noise, the correlation between GFP and RFP was analysed (see supplementary data, figure S4: stacks.iop.org/PhysBio/6/036015). The estimated intrinsic noise (figure 7, broken lines) was consistent to the inherent part of the total noise (figure 7, solid curves) that estimated from the dependence of CV on the mean GFP concentration. We estimated the threshold where noise in the cell growth rate and intrinsic noise contribute equally.

The contribution of intrinsic noise, $CV_{x,\text{int}}$, is estimated as $\sqrt{\frac{b}{\langle x \rangle}}$ shown in equation (A.5.3) and (S18: stacks.iop.org/PhysBio/6/036015). The coefficient b is called as burst size and represents the number of protein synthesized from a single mRNA within the lifetime of the mRNA. The contribution of noise in the cell growth rate, CV_{x,ext_μ}, is estimated as follows, where fast noise limit is used as shown in equation (S13: stacks.iop.org/PhysBio/6/036015):

$$CV_{x,\text{ext}_\mu} = \sqrt{\frac{D_\mu}{\mu_0 - D_\mu}} \approx CV_\mu, \qquad \mu_0 \gg D_\mu,$$

where CV_μ represents CV of the distribution of the cell growth rate. In the case of $CV_{x,\text{ext}_\mu} > CV_{x,\text{int}}$ the following estimation is induced:

$$\frac{\langle x \rangle}{b} > \frac{1}{CV_\mu^2},$$

where $\frac{\langle x \rangle}{b}$ represents the number of mRNA synthesized within a generation (see the supplementary data and equations (S37) and (S66): stacks.iop.org/PhysBio/6/036015). For instance, 50 molecules of mRNA per generation are the threshold estimated in this study. It indicates that noise in the cell growth rate contributes to the fluctuation in GFP concentration more than noise in the protein synthesis rate does, when the expression level is higher than 50 mRNA molecules per cell.

Global properties of noise in the cell growth rate

Thus far, fluctuations in gene copy number, chromosomal position of the gene, particular transcriptional networks, etc, have been identified as the origins of extrinsic noise [6, 29, 40]. Variation in these factors specifically affects the fluctuation of the expression of target genes, but not that of all genes in the cell. In contrast, our proposal that noise in the cell growth rate is a powerful cause of fluctuation in cell protein concentration points to a fundamental property of global noise. As the cell growth rate is a global parameter characterizing dilution throughout the cell, noise in the cell growth rate potentially influences fluctuations in the concentrations of all cellular components, acting as global noise.

To verify this proposition, we estimated the fluctuation in concentration of RFP, co-expressed with the TetR repressor protein. The characteristics of extrinsic noise depend not only on the network architecture but also on the gene expression level (concentration of the inducer) [13, 29]. According to the schematic design of our genetic circuit, GFP and RFP concentrations may be negatively correlated if noise in the TetR repressor concentration is transmitted to the expression of GFP. This property has been confirmed at low concentrations of IPTG [29]. However, because RFP (as well as TetR) is fully expressed by adding a sufficient amount of IPTG and because noise in transcription and translation has a time scale (~10 min) [32] that is shorter than the lifespan of GFP (~10 h) [3, 38], the transmitted noise is ignored, and the network-independent noise dominates instead (see supplementary data: stacks.iop.org/PhysBio/6/036015) [29]. Indeed, the correlation between GFP and RFP concentrations is not negative but positive (figure S2: stacks.iop.org/PhysBio/6/036015). Moreover, the total fluctuation in RFP concentration was found to be approximately equal to that in GFP concentration (figure S6: stacks.iop.org/PhysBio/6/036015). Hence, noise in the cell growth rate is likely to perturb GFP and RFP concentrations in the same manner. In particular, at a high expression level, the ratio of the correlation between the two protein concentrations rose from 0.31 to 0.74 as the gene products accumulated (figure S2: stacks.iop.org/PhysBio/6/036015). In addition, other factors such as ribosomes and network-independent transcription factors might be considered as the

dominant sources of extrinsic noise that act globally on the genome-wide gene expression. Unlike these extrinsic noises, noise in the cell growth rate disturbs not only the concentration of the entire set of gene products (proteins) but also all cellular components, resulting in synchronized phenotypic fluctuation.

Conclusion and outlook

Using a genetic circuit and a dynamic model, we evaluated precisely the contribution of noise in the cell growth rate to the fluctuation in cell protein concentration particularly for fast growing bacterial cells. The theoretical model used here was experimentally verified to show that it captured the dynamics of cell protein concentration (figure 4, see supplementary data: stacks.iop.org/PhysBio/6/036015) and precisely explained the well-known properties of cell protein concentration, the right-tailed distribution and the average-independent CV (figure 6, see supplementary data: stacks.iop.org/PhysBio/6/036015). The model shows that noise in the cell growth rate acts as a source of extrinsic noise and can simply be introduced into the dynamic model for the quantitative prediction of its dominant contribution to the fluctuating protein concentration. Consequently, noise in the cell growth rate, demonstrated in this investigation by time-lapse microscopy (figure 5), was found to contribute to extrinsic noise, accounting for dozens of percent (figure 7).

How do bacterial cells tolerate large fluctuations in cellular components? If all cellular components show large fluctuations of similar magnitude, the protein networks of the cell might show considerable disturbance. A proportion of cell proteins is crucially controlled by local regulatory mechanisms, such as those controlled by operons, regulons and target-specific degradation, to adjust their cellular concentration and maintain homeostasis. However, most proteins in bacterial cells are synthesized constitutively, degraded slowly [25] and diluted by cell growth. Consequently, their concentrations are inevitably perturbed by noise in the cell growth rate. However, the global nature of fluctuation in cellular component concentrations induced by noise in the cell growth rate may preserve the relative amounts of all cellular components. Thus, a large but coherent fluctuation in these components may contribute greatly to the stability of the intact cellular network, and accordingly provide phenotypic diversity at a level that would sustain growing systems in a fluctuating environment [1].

Acknowledgments

Appendix

In previous studies [13, 26, 29, 37], the stochastic nature of protein concentration was characterized successfully by the Langevin equation, in which noise terms are added to the deterministic equation as follows:

$$\frac{\mathrm{d}x}{\mathrm{d}t} = k_x - \mu_0 x + \sqrt{D_{x,\mathrm{int}}}\eta_{x,\mathrm{int}}(t) + \sqrt{D_{x,\mathrm{ext}}}\eta_{\mathrm{ext}}(t), \quad \text{(A.1)}$$

where $\eta_{x,\mathrm{int}}(t)$ and $\eta_{\mathrm{ext}}(t)$ represent intrinsic and extrinsic noises, respectively. The diffusion constants are generally defined as follows:

$$D_{x,\mathrm{int}} = b\mu_0\langle x\rangle, \quad \text{(A.2.1)}$$

$$D_{x,\mathrm{ext}} = c\mu_0\langle x\rangle^2. \quad \text{(A.2.2)}$$

Equation (A.2.1) is derived from the Poisson-like stochastic process and has been verified theoretically and experimentally [13, 15, 26, 41]. Because of its unspecified origin, equation (A.2.2) is constructed phenomenologically from the evidence, particularly in the case of global noise [13, 26, 29], and plays a multiplicative role, as follows:

$$\frac{\mathrm{d}x}{\mathrm{d}t} = k_x - \mu_0 x + \sqrt{b\mu_0\langle x\rangle}\eta_{x,\mathrm{int}}(t) + \langle x\rangle\sqrt{c\mu_0}\eta_{\mathrm{ext}}(t).$$

$$\text{(A.3)}$$

Although the multiplicative stochastic property of the unknown extrinsic noise can be described as $D_{x,\mathrm{ext}} = c\mu_0 x^2$, not $D_{x,\mathrm{ext}} = c\mu_0\langle x\rangle^2$, we note that the difference between these interpretations poses little problem for the analysis of the mean or variance.

In spite of the slow time scale of the noises [4, 32, 35], the variance and the mean at the steady state are roughly time independent [13]. Thus, the white noise limit is applied here:

$$\langle\eta_j(t)\rangle = 0, \quad \text{(A.4.1)}$$

$$\langle\eta_j(t)\eta_j(t')\rangle = 2\delta(t - t') \qquad j \in \mathrm{int}, \mathrm{ext}, \quad \text{(A.4.2)}$$

where δ is the delta function.

Subsequently, the average $\langle x\rangle$, the standard deviation σ_x and the coefficient of variation CV_x are calculated as follows:

$$\langle x\rangle = \frac{k_x}{\mu_0}, \quad \text{(A.5.1)}$$

$$\sigma_x = \sqrt{b\langle x\rangle + c\langle x\rangle^2}, \quad \text{(A.5.2)}$$

$$CV_x = \frac{\sigma_x}{\langle x\rangle} = \sqrt{\frac{b}{\langle x\rangle} + c}. \quad \text{(A.5.3)}$$

Equation (A.5.2) is introduced according to the standard procedure as described previously [29, 37]. Equation (A.5.3) reveals the relationship between the CV of protein concentration and the mean $\langle x\rangle$. CV_x comprises both a Poisson-like statistical property from intrinsic noise ($\sqrt{\frac{b}{\langle x\rangle}}$ in equation (A.5.3)) and an invariable feature from extrinsic noise ($\sqrt{c}$ in equation (A.5.3)). Apparently, the fluctuation in protein concentration (CV_x) declines when the mean concentration ($\langle x\rangle$) increases, but reaches a constant value when intrinsic noise turns to negligible along with the increase in the

mean. Such constant fluctuation is derived from extrinsic noise, which acts in a multiplicative manner, as shown in equation (A.3): $\langle x \rangle \sqrt{c\mu_0} \eta_{\text{ext}}(t)$. Equation (A.5.3) is used to estimate the contribution of extrinsic noise $\sqrt{c}$ after obtaining the contribution of intrinsic noise by the experiment detailed in the results and discussion section (figure 7).

References

[1] Acar M, Mettetal J T and van Oudenaarden A 2008 Stochastic switching as a survival strategy in fluctuating environments *Nat. Genet.* **40** 471–5

[2] Alon U 2007 *An Introduction to Systems Biology: Design Principles of Biological Circuits* (London: Chapman and Hall)

[3] Andersen J B, Sternberg C, Poulsen L K, Bjorn S P, Givskov M and Molin S 1998 New unstable variants of green fluorescent protein for studies of transient gene expression in bacteria *Appl. Environ. Microbiol.* **64** 2240–6

[4] Austin D W, Allen M S, McCollum J M, Dar R D, Wilgus J R, Sayler G S, Samatova N F, Cox C D and Simpson M L 2006 Gene network shaping of inherent noise spectra *Nature* **439** 608–11

[5] Bar-Even A, Paulsson J, Maheshri N, Carmi M, O'Shea E, Pilpel Y and Barkai N 2006 Noise in protein expression scales with natural protein abundance *Nat. Genet.* **38** 636–43

[6] Becskei A, Kaufmann B B and van Oudenaarden A 2005 Contributions of low molecule number and chromosomal positioning to stochastic gene expression *Nat. Genet.* **37** 937–44

[7] Bevis B J and Glick B S 2002 Rapidly maturing variants of the Discosoma red fluorescent protein (DsRed) *Nat. Biotechnol.* **20** 83–7

[8] Bouvier T, Troussellier M, Anzil A, Courties C and Servais P 2001 Using light scatter signal to estimate bacterial biovolume by flow cytometry *Cytometry* **44** 188–94

[9] Cai L, Friedman N and Xie X S 2006 Stochastic protein expression in individual cells at the single molecule level *Nature* **440** 358–62

[10] Datsenko K A and Wanner B L 2000 One-step inactivation of chromosomal genes in Escherichia coli K-12 using PCR products *Proc. Natl. Acad. Sci. USA* **97** 6640–5

[11] Dunlop M J, Cox R S III, Levine J H, Murray R M and Elowitz M B 2008 Regulatory activity revealed by dynamic correlations in gene expression noise *Nat. Genet.* **40** 1493–8

[12] Elowitz M B and Leibler S 2000 A synthetic oscillatory network of transcriptional regulators *Nature* **403** 335–8

[13] Elowitz M B, Levine A J, Siggia E D and Swain P S 2002 Stochastic gene expression in a single cell *Science* **297** 1183–6

[14] Furusawa C, Suzuki T, Kashiwagi A, Yomo T and Kaneko K 2005 Ubiquity of log-normal distributions in intra-cellular reaction dynamics *Biophysics* **1** 25–31

[15] Golding I, Paulsson J, Zawilski S M and Cox E C 2005 Real-time kinetics of gene activity in individual bacteria *Cell* **123** 1025–36

[16] Ito Y, Kawama T, Urabe I and Yomo T 2004 Evolution of an arbitrary sequence in solubility *J. Mol. Evol.* **58** 196–202

[17] Kaneko K and Yomo T 1999 Isologous diversification for robust development of cell society *J. Theor. Biol.* **199** 243–56

[18] Kashiwagi A, Sakurai T, Tsuru S, Ying B W, Mori K and Yomo T 2009 Construction of *Escherichia coli* gene expression level perturbation collection *Metab. Eng.* **11** 56–63

[19] Kashiwagi A, Urabe I, Kaneko K and Yomo T 2006 Adaptive response of a gene network to environmental changes by fitness-induced attractor selection *PLoS. ONE* **1** e49

[20] Ko M S, Nakauchi H and Takahashi N 1990 The dose dependence of glucocorticoid-inducible gene expression results from changes in the number of transcriptionally active templates *EMBO. J.* **9** 2835–42

[21] Korobkova E, Emonet T, Vilar J M, Shimizu T S and Cluzel P 2004 From molecular noise to behavioural variability in a single bacterium *Nature* **428** 574–8

[22] Krishna S, Banerjee B, Ramakrishnan T V and Shivashankar G V 2005 Stochastic simulations of the origins and implications of long-tailed distributions in gene expression *Proc. Natl. Acad. Sci. USA* **102** 4771–6

[23] Maamar H, Raj A and Dubnau D 2007 Noise in gene expression determines cell fate in Bacillus subtilis *Science* **317** 526–9

[24] McAdams H H and Arkin A 1997 Stochastic mechanisms in gene expression *Proc. Natl. Acad. Sci. USA* **94** 814–9

[25] Nath K and Koch A L 1970 Protein degradation in *Escherichia coli*: I. Measurement of rapidly and slowly decaying components *J. Biol. Chem.* **245** 2889–900

[26] Newman J R, Ghaemmaghami S, Ihmels J, Breslow D K, Noble M, DeRisi J L and Weissman J S 2006 Single-cell proteomic analysis of *S. cerevisiae* reveals the architecture of biological noise *Nature* **441** 840–6

[27] Ozbudak E M, Thattai M, Kurtser I, Grossman A D and van Oudenaarden A 2002 Regulation of noise in the expression of a single gene *Nat. Genet.* **31** 69–73

[28] Paulsson J 2005 Prime movers of noisy gene expression *Nature. Genet.* **37** 925?6

[29] Pedraza J M and van Oudenaarden A 2005 Noise propagation in gene networks *Science* **307** 1965–9

[30] Raser J M and O'Shea E K 2004 Control of stochasticity in eukaryotic gene expression *Science* **304** 1811–4

[31] Rosenfeld N, Elowitz M B and Alon U 2002 Negative autoregulation speeds the response times of transcription networks *J. Mol. Biol.* **323** 785–93

[32] Rosenfeld N, Young J W, Alon U, Swain P S and Elowitz M B 2005 Gene regulation at the single-cell level *Science* **307** 1962–5

[33] Sato K, Ito Y, Yomo T and Kaneko K 2003 On the relation between fluctuation and response in biological systems *Proc. Natl. Acad. Sci. USA* **100** 14086–90

[34] Shahrezaei V, Ollivier J F and Swain P S 2008 Colored extrinsic fluctuations and stochastic gene expression *Mol. Syst. Biol.* **4** 196

[35] Sigal A, Milo R, Cohen A, Geva-Zatorsky N, Klein Y, Liron Y, Rosenfeld N, Danon T, Perzov N and Alon U 2006 Variability and memory of protein levels in human cells *Nature* **444** 643–6

[36] Suel G M, Kulkarni R P, Dworkin J, Garcia-Ojalvo J and Elowitz M B 2007 Tunability and noise dependence in differentiation dynamics *Science* **315** 1716–9

[37] Thattai M and van Oudenaarden A 2001 Intrinsic noise in gene regulatory networks *Proc. Natl. Acad. Sci. USA* **98** 8614–9

[38] Tombolini R, Unge A, Davey M E, Bruijn F J and Jansson J K 1997 Flow cytometric and microscopic analysis of GFP-tagged pseudomonas fluorescens bacteria *FEMS. Microbiol. Ecol.* **22** 17–28

[39] Trueba F J and Woldringh C L 1980 Changes in cell diameter during the division cycle of *Escherichia coli J. Bacteriol.* **142** 869–78

[40] Volfson D, Marciniak J, Blake W J, Ostroff N, Tsimring L S and Hasty J 2006 Origins of extrinsic variability in eukaryotic gene expression *Nature* **439** 861–4

[41] Yu J, Xiao J, Ren X, Lao K and Xie X S 2006 Probing gene expression in live cells, one protein molecule at a time *Science* **311** 1600–3